JOURNAL OF GEOPHYSICAL RESEARCH, VOL. 99, NO. C9, PAGES 18,371–18,384, SEPTEMBER 15, 1994

Seasonal and interannual variability of coastal zone color scanner phytoplankton pigments and winds in the eastern tropical Pacific

Paul C. Fiedler

National Marine Fisheries Service, Southwest Fisheries Science Center, La Jolla, California

Abstract. Time series of phytoplankton pigment concentration along coastal and oceanic transects in the eastern tropical Pacific Ocean were derived from coastal zone color scanner monthly composite data for November 1978 through June 1986. Seasonal and interannual variability made up about half the total variance of the time series. Seasonal cycles typically consisted of a spring minimum and fall maximum, although many local variations were observed. Interannual variability was as great as seasonal variability and was dominated by the 1982-1983 El Niño event. The decline in pigment concentration during 1983 was less to the west of the Galapagos than to the east and along the Central American coast. Physical forcing of pigment variability was investigated by testing correlations between pigment concentration and wind variables associated with upwelling and mixing. Seasonal cycles and some interannual changes in pigment concentration were correlated with local wind-driven processes that cause variation in primary productivity. Correlations between pigments and local winds in oceanic transects were different at seasonal and interannual scales, implying remote forcing at the interannual timescale.

Introduction

The eastern tropical Pacific Ocean (ETP) (Figure 1) is subject to strong interannual forcing associated with the El Niño-Southern Oscillation. This variability affects phytoplankton production and the survival and reproduction of organisms at higher trophic levels [*Barber and Chavez*, 1986]. Biological effects of interannual variability have been inferred from limited field observations and fishery catch data [*Glynn*, 1990]. For example, *Cowles et al.* [1977] described reduced nutrient content and primary productivity in surface waters between the Galapagos and the coast of Ecuador and northern Peru during the 1975 El Niño. *Schreiber and Schreiber* [1984] reported adult mortality and reproductive failure of seabirds on Christmas Island, and *Trillmich and Limberger* [1985] documented mortality of pinnipeds on the Galapagos during the 1982-1983 event. *Valdivia* [1978] reviewed changes in the Peruvian anchoveta stock during the 1972 El Niño, while noting the problem of separating environmental from man-induced effects on heavily exploited living resources. Taken together, such reports show widespread and pervasive biological effects of El Niño in the ETP.

Seasonal variability of physical variables (surface temperature, mixed layer depth, thermocline depth, and wind stress) equals or exceeds interannual variability in large parts of the ETP [*Fiedler*, 1992; *Delcroix*, 1993]. Thus we cannot assume that the interannual scale is the only important scale of biological variability in this low-latitude ecosystem. Sampling by shipboard surveys has not been adequate to describe seasonal cycles or interannual variability of phytoplankton biomass or production, except in limited regions [*Rojas de Mendiola*, 1981] or for single events [*Fiedler et al.*, 1992]. *Dessier and Donguy* [1985] demonstrated seasonal cycles of surface chlorophyll concentration and copepod abundance in the eastern tropical Pacific from an exceptional time series of samples collected in the ship-of-opportunity program Surveillance Trans-Océanique du Pacifique (SURTROPAC). *Dandonneau* [1992] analyzed seasonal and interannual variability of surface chlorophyll concentration in the tropical Pacific from 1978-1989 SURTROPAC results. This analysis was complicated by (1) irregular sampling intervals, which necessitated interpolation and smoothing of the time series, and (2) spatial variability of the ship tracks, which appeared as temporal variability at a given latitude (for example, the "eastern Pacific" transect crossed the equator from 0 to 2000 km west of the Galapagos in a strong longitudinal chlorophyll gradient).

Satellite sensors can potentially provide data with spatially and temporally uniform coverage that are ideal for time series analysis. The coastal zone color scanner (CZCS) aboard the Nimbus 7 satellite collected visible radiance data from November 1978 through June 1986. Unfortunately, CZCS coverage was far from complete over most of the global ocean. Nevertheless, this instrument has provided the best temporal and spatial coverage available for estimates of phytoplankton pigment concentration in remote regions. *Feldman et al.* [1984] and *Feldman* [1986] showed that near-surface phytoplankton pigment concentration estimated from CZCS radiance data could be used to quantify the effects of El Niño in the eastern equatorial Pacific. *Strub et al.* [1990] used CZCS data to show relationships between phytoplankton pigment concentration and winds in the California Current, one of the regions most completely covered by the CZCS. *Thomas et al.* [1994] attempted to extend that analysis to the Peru Current region but found that coverage was inadequate. In this paper I analyze the CZCS data set for temporal and spatial variability of phytoplankton pigment concentration in well-covered areas of the ETP. Relationships with wind-driven processes are examined

Paper number 94JC01807.

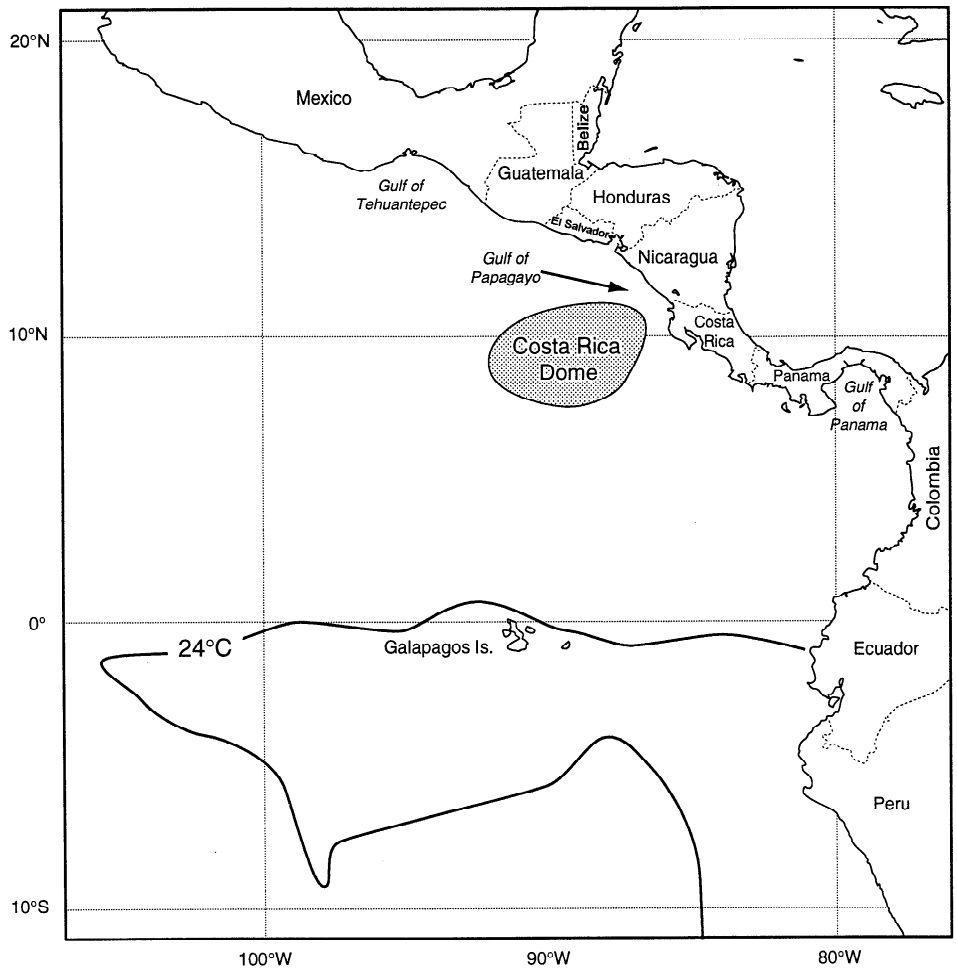

Figure 1. Map of study area in the eastern tropical Pacific Ocean. The 24°C isotherm defines the equatorial cold tongue.

by testing correlations of pigments with alongshore and offshore wind stress along the coast and with wind stress and Ekman pumping (upwelling) in the open ocean.

Methods

Monthly composites of CZCS phytoplankton pigment concentration were obtained from NASA Goddard Space Flight Center. These data are now available on CD-ROM (NASA Jet Propulsion Laboratory, Physical Oceanography Distributed Active Archive Center, Pasadena, California). Image files were manipulated using SEAPAK software [*McClain et al.*, 1992]. All data analysis was done with the pigment estimates in the original log-transformed scaling, thus the mean values reported here are geometric means. The image files were sampled to compute monthly averages of CZCS pigment concentration in 1° squares along one coastal and three oceanic transects (Figure 2) as follows: (1) coastal, along the Central American coast from central Mexico to Panama, (2) countercurrent, along the countercurrent divergence at 9°N, between the North Equatorial Current and the North Equatorial Countercurrent, (3) equatorial, along the cold tongue of equatorial surface water, and (4) 95°W, from the Gulf of Tehuantepec to the south across the countercurrent divergence and equatorial cold tongue. These transects were selected to cover interesting regions where data were obtained during at least 30 months of the 92-month lifetime of the CZCS. Monthly coverage (months with data from at least one pass) along these transects was only 60%, on average (Figure 3). Incomplete coverage was typical of most regions in the global data set, owing to the limited availability of recorder time on the Nimbus 7 satellite. In the ETP, coverage was nearly complete during 1979, but gaps of 1-4 months were typical during summer in subsequent years. This pattern was imposed by the duty cycle of the sensor rather than by seasonal cloudiness, based on examination of individual monthly composites.

The resolution of the global monthly composites is about 18 km near the equator, so each 1° square contained 36 pixels. A monthly mean was calculated only if at least 10% (four) of the pixels in a square had valid data. Each monthly time series contained variability on interannual (> 1 year) and seasonal (< 1 year) timescales. The total variance of each time series was partitioned by (1) applying a double 13-month running mean to extract the interannual component and (2) calculating monthly means of the residuals from the running mean to extract the seasonal component. Thus "seasonal" variability is the variability between monthly means. Residuals from the seasonal cycle represent month-to-month variability that was considered to be noise and remained "unexplained" in this study.

Wind variables were derived from Comprehensive Ocean-Atmosphere Data Set (COADS) interim Compressed Marine

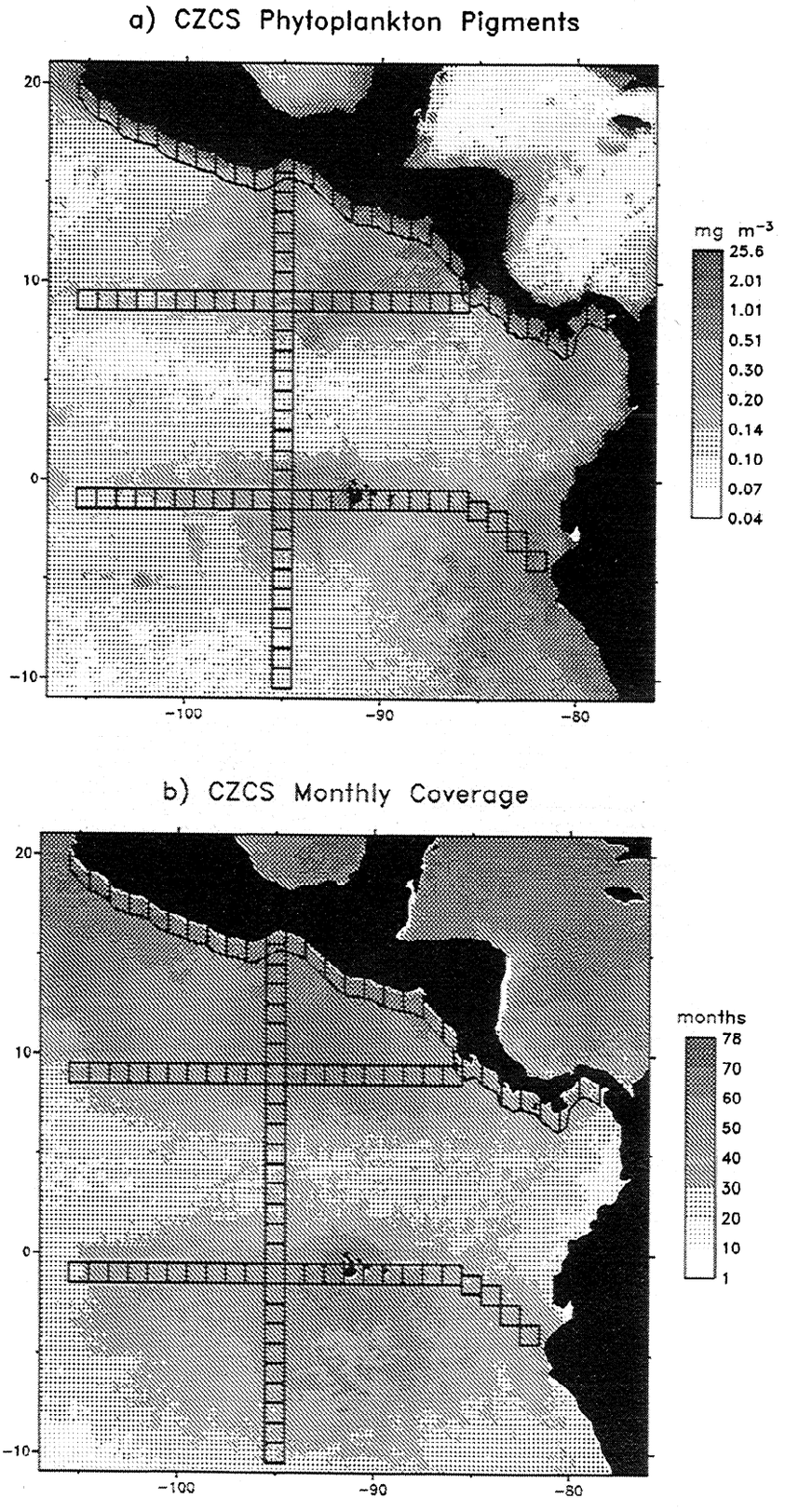

Figure 2. (a) Mean coastal zone color scanner (CZCS) phytoplankton pigment concentration (in milligrams per cubic meter) and (b) monthly CZCS coverage (months out of 92) from November 1978 through June 1986. Squares are the 1° squares in which monthly means were calculated for the analysis of seasonal and interannual variability.

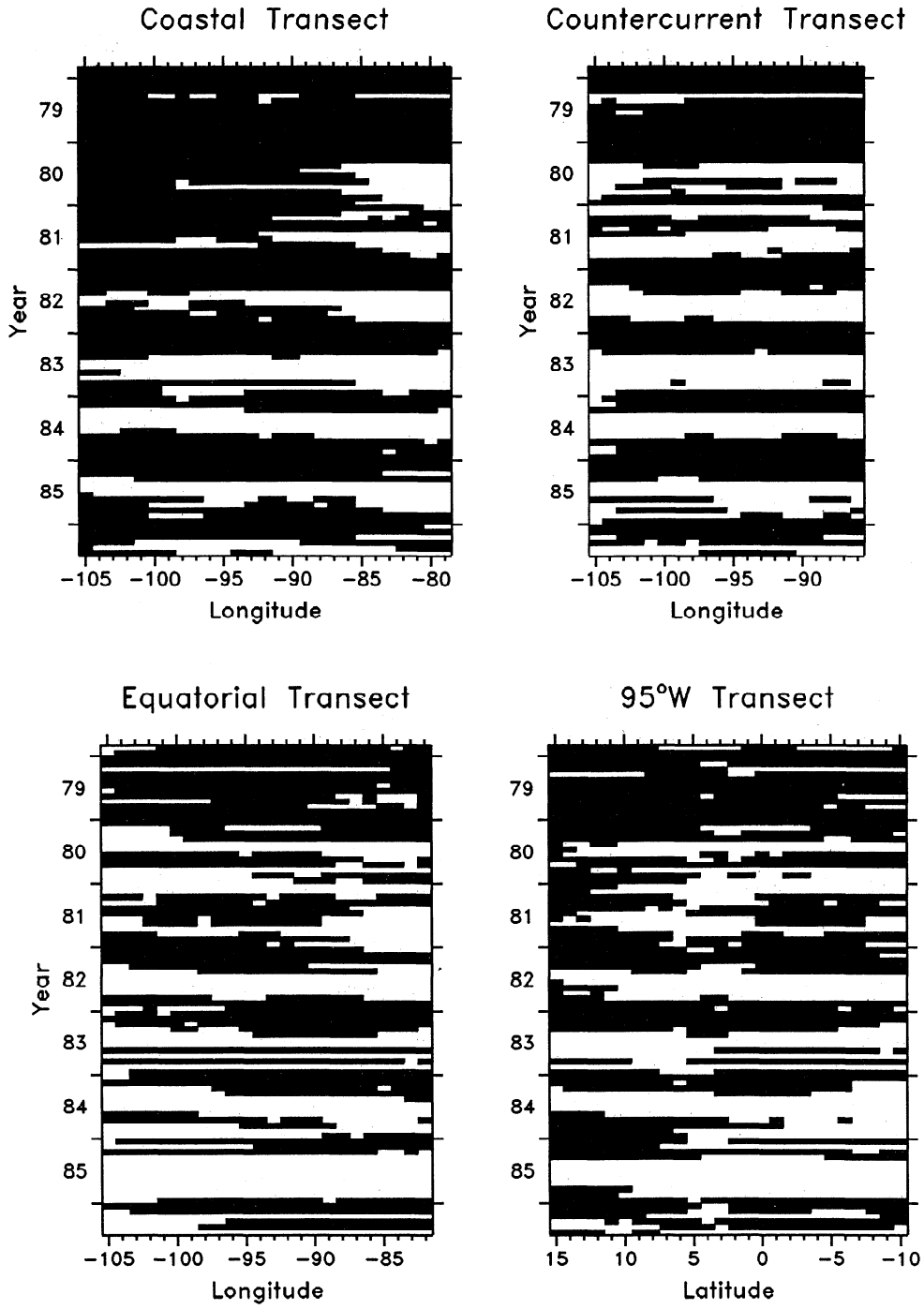

Figure 3. Months for which mean CZCS phytoplankton pigment concentration could be calculated (black) in 1° squares along coastal, countercurrent, equatorial, and 95°W transects in the eastern tropical Pacific.

Reports of vector wind observations [*Woodruff et al.*, 1987]. For the coastal transect, wind observations were binned in the same 1° squares as CZCS pigments. For the oceanic transects, where wind observations were more sparse, a weighted monthly mean of observations within a distance of 2° from the center of each 1° square was calculated. Wind velocity was converted to wind stress (τ, N m^{-2}) using an air density of 1.2 kg m^{-3} and a drag coefficient equal to 1.2 x 10^{-3} for wind speeds <11 m s^{-1} and increasing by 0.065 x 10^{-3} (m s^{-1})$^{-1}$ for stronger winds [*Large and Pond*, 1981]. In the coastal transect, wind stress vectors were rotated to alongshore τ_a (positive equals equatorward) and offshore τ_o components. Equatorward, alongshore wind stress drives offshore Ekman transport of surface waters, resulting in coastal upwelling.

In the oceanic transects, total wind stress τ was calculated from the COADS wind velocity components as a measure of the flux of wind energy driving vertical mixing beneath the sea surface. Ekman pumping velocity w_E was calculated from the divergence of horizontal Ekman transports (U, V) calculated as:

$$U = (\delta\tau_x + f\tau_y) / [\rho(f^2 + \delta^2)],$$

$$V = (\delta\tau_y - f\tau_x) / [\rho(f^2 + \delta^2)],$$

where τ_x and τ_y are the eastward and northward components of wind stress, respectively, ρ is water density (10^3 kg m^{-3}), f is the Coriolis parameter ($2\Omega \sin \phi$), and δ is a frictional damping parameter [$\delta = (4.8\ \mathrm{d})^{-1}$] which balances wind forcing near the equator where f vanishes [*Hsieh and Boer*, 1992]. Thus w_E is an estimate of wind-driven oceanic upwelling, even at the equator. The temporal and spatial smoothing involved in gridding the wind vector data reduce the estimated magnitude of Ekman upwelling or downwelling.

Monthly time series of the two coastal (τ_a, τ_n) and two oceanic (τ, w_E) wind variables were analyzed as above to isolate interannual and seasonal variability. Correlations between pigment concentrations and wind variables were calculated using the interannual and seasonal components of the time series. Pigment-wind correlations were also calculated with pigments lagged by 1 month; the value reported here is the unlagged or lagged correlation with the greatest absolute value. *Chelton* [1982] warned that strong narrowband signals, such as seasonal cycles, can reduce the true degrees of freedom in statistical analyses of time series. The total degrees of freedom (range 35 to 76) were partitioned to give 7 d.f. (92/13) for the interannual correlations and 4 d.f. for the seasonal correlations. Seasonal cycles are typically well described by annual and semiannual harmonics. The assigned degrees of freedom represent the amplitudes and phases of the two harmonics.

Results

The total variance of monthly mean CZCS pigment concentration included, on average, 25% seasonal and 27% interannual variance (Table 1). Seasonal cycles, year-to-year variability, and local centers of high pigment concentration were revealed by partitioning the data (Figures 4-7), which removed the unexplained "noise" and smoothed the gaps in the data.

The coastal transect had high pigment concentrations at the three following locations: the Gulf of Tehuantepec at 95°W, the Gulf of Papagayo at 86°W, and the Gulf of Panama at 79°W (Figure 4). Pigment concentration increased from west to east along the countercurrent transect, with a maximum near 89°W at the Costa Rica Dome (Figure 5). Pigment concentration also increased from west to east along the equatorial transect, except for a local maximum off the western side of the Galapagos at 91°W (Figure 6). Highest concentrations were found at the eastern end of the transect, about 100 km off the coast of Ecuador. Along the 95°W transect, pigment concentration was highest at 15°N, near the Gulf of Tehuantepec (Figure 7). To the south, two maxima of similar magnitude were centered at 9°N and 1°S (see also Figure 2).

Seasonal Variability

Month-longitude (or latitude-month) plots of mean pigment concentration, with the interannual variability removed, illustrate seasonal cycles for the 1978-1986 period (top left panels in Figures 4-7). Pigment concentration at many locations was minimum in boreal spring (March-May) and maximum in late summer or fall (August-November); that is, there was a single, fall bloom. There were numerous variations on this pattern.

Along the coastal transect, in the central Mexico region (105-100°W), pigment concentration was maximum in spring, with a secondary fall maximum (Figure 4). At the Gulf of Tehuantepec (95°W) the seasonal maximum occurred in early winter (November-January). To the east there was a single late summer or fall maximum, except at the Gulfs of Papagayo (86°W) and Panama (79°W), where a secondary maximum occurred in winter-spring.

Table 1. Seasonal and Interannual Variances (Divided by Total Variance) of Monthly Mean CZCS Phytoplankton Pigment Concentration and Wind Stress Along Coastal, Countercurrent, Equatorial, and 95°W Transects in the Eastern Tropical Pacific, November 1978 - June 1986.

	Pigment		Wind	
	Seasonal	Interannual	Seasonal	Interannual
Coastal	.26	.27	.31	.11
Countercurrent	.25	.34	.49	.06
Equatorial	.24	.25	.34	.17
95°W	.21	.25	.43	.08
Average	.25	.27	.39	.11

Along the countercurrent transect (Figure 5) the seasonal cycle consisted of a spring minimum and fall maximum, except at the Costa Rica Dome (89°W), where a secondary spring bloom occurred. The typical seasonal cycle (spring minimum, fall maximum) occurred all along the equatorial transect (Figure 6), except near the coast of Ecuador (82°W), where the boreal fall bloom persisted through winter and the seasonal minimum occurred in June. The 95°W transect showed the typical seasonal cycle at all latitudes (Figure 7). Seasonal variability was very low between 2°N and 6°N and south of 5°S.

Interannual Variability

The 13-month running mean filled the gaps in the time series. The resulting fields show patterns of interannual variability that are highly coherent throughout the ETP (bottom left panels in Figures 4-7). However, these patterns are valid only at an interannual timescale. Apparent phase differences of a few months may be artifacts of smoothing the gappy time series.

Pigment concentration increased gradually during 1979 and 1980 and reached a maximum during 1981. A subsequent decline led to minimum pigment concentrations throughout the ETP during the 1982-1983 El Niño. The only exception to this pattern was along the equatorial transect west of 96°W, where a 1983 minimum was not apparent. Along the 95°W transect the minimum occurred during winter 1982-1983 at the equator and then progressively later to the north and south, except near the coast at the Gulf of Tehuantepec. This pattern is significant because the phase shift is coherent from the equator to at least 10°N (and S), where the minimum occurred 1 year later than at the equator.

The decline in mean pigment concentration during El Niño 1982-1983 averaged 39% (range 5%-69%) in the smoothed monthly time series (Figure 8). The percentage decline increased from west to east along both the countercurrent transect and the equatorial transects and increased from the equator to the north and to the south along the 95°W transect.

Recovery of pigment concentrations to pre-El Niño levels occurred during 1984 throughout the region. In some areas, including the Gulf of Papagayo (Figure 4), Costa Rica Dome

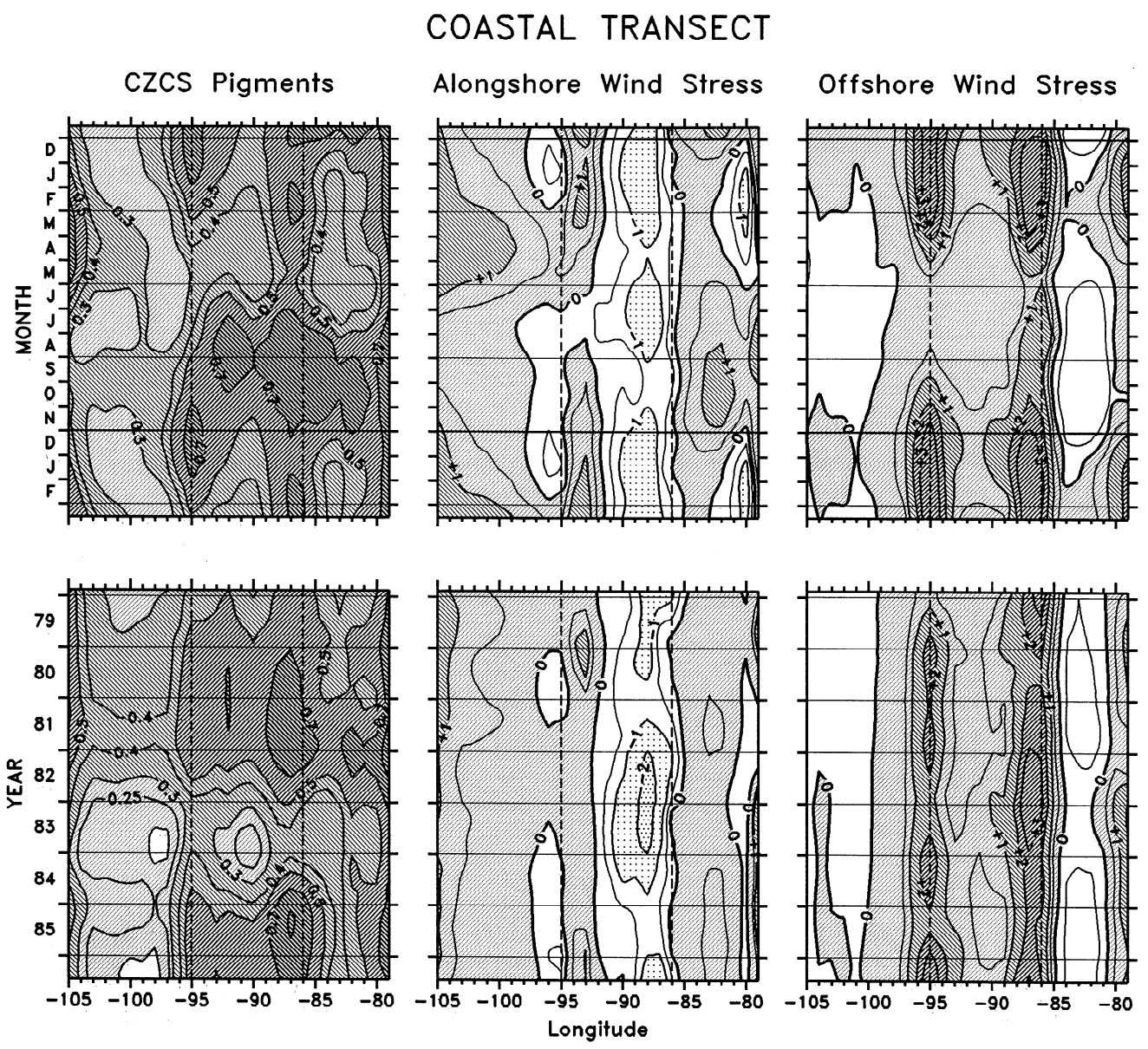

Figure 4. (top) Seasonal (mean residuals from double 13-month running mean) and (bottom) interannual (double 13-month running mean) variability of monthly mean CZCS phytoplankton pigment concentration (in milligrams per cubic meter) and alongshore and offshore wind stress (10^{-2} N m^{-2}) in 1° squares along the coastal transect. Dashed lines mark the Gulf of Tehuantepec at 95°W and the Gulf of Papagayo at 86°W. The Gulf of Panama is at 79°W.

(Figure 5) and the Galapagos (Figure 6), maximum pigment levels reached during 1985 exceeded the maximum pre-El Niño levels. Pigment concentrations were declining during the first half of 1986, when the CZCS ceased operation.

Pigment-Wind Relationships

Surface winds in the tropics form two bands, the northeast and southeast trade winds, which converge at or near the equator in the intertropical convergence zone (ITCZ). Monthly mean wind velocities (Figure 9) show variations of this pattern in the eastern tropical Pacific. The SE trade winds blow year-round south of 4°N. North of the equator, however, these winds are more southerly to the west of the Galapagos and southwesterly to the east. The NE trade winds blow year-round north of 16°N, although they are northwesterly (alongshore) near the coast of central Mexico. Between 4°N and 16°N the trade winds reverse seasonally owing to migration of the ITCZ. This seasonality is most pronounced at 7-9°N, the mean position of the ITCZ in this region. Here the trade winds are northeasterly during winter, when the ITCZ is to the south, and southwesterly during summer, when the ITCZ is to the north.

Time series of pigment concentration and wind stress had different relative proportions of seasonal and interannual variance (Table 1). For pigments, interannual variance was approximately equal to seasonal variance. In contrast, seasonal variance of wind stress exceeded interannual variance by at least a factor of 3, except along the equatorial transect. Seasonality of winds was much greater along the countercurrent

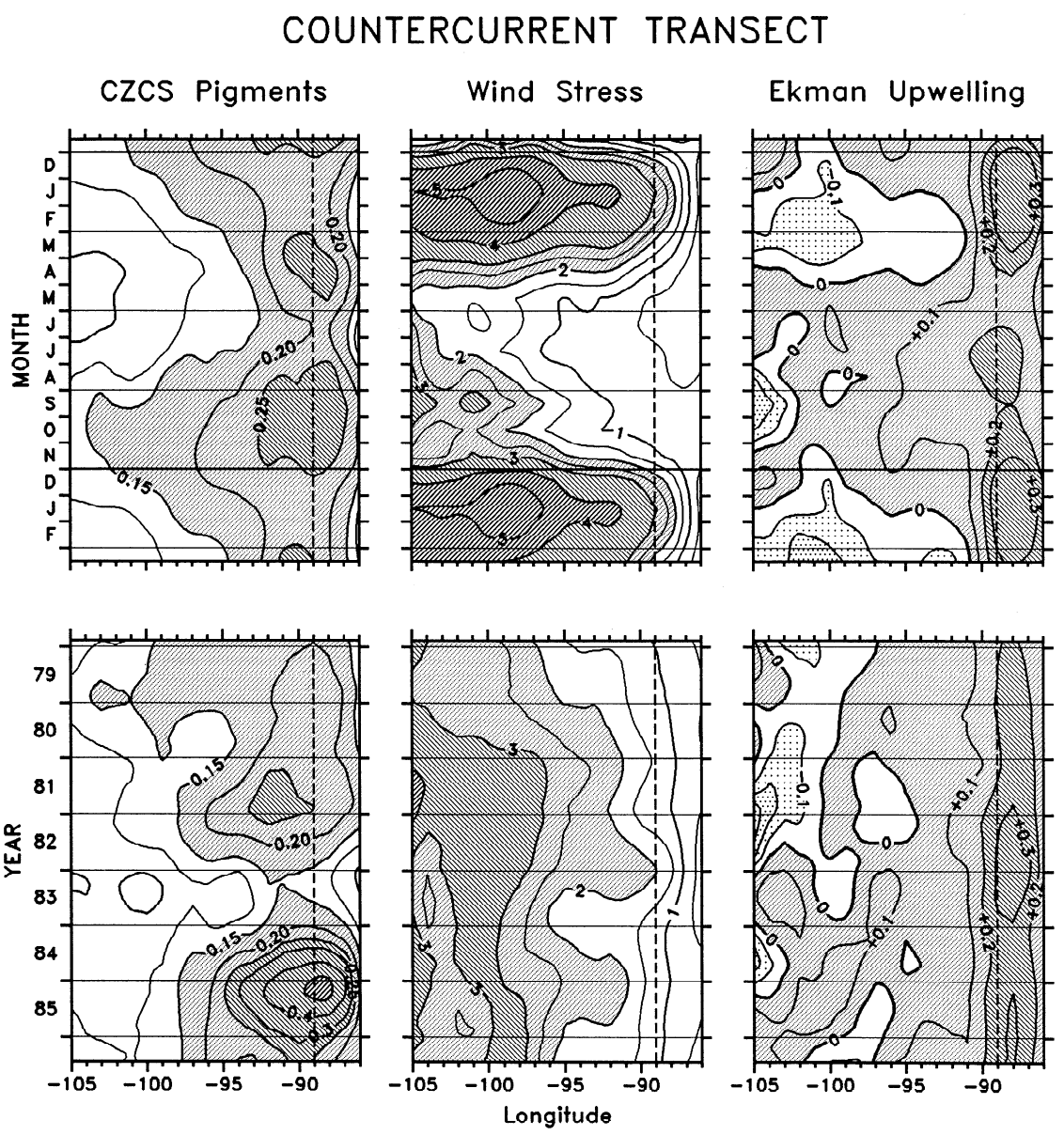

Figure 5. (top) Seasonal (mean residuals from double 13-month running mean) and (bottom) interannual (double 13-month running mean) variability of monthly mean CZCS phytoplankton pigment concentration (in milligrams per cubic meter), wind stress (10^{-2} N m^{-2}), and Ekman upwelling velocity (10^{-5} m s^{-1}) in 1° squares along the countercurrent transect. Dashed line marks the Costa Rica Dome at 89°W.

transect, under the ITCZ, than along the equatorial transect. On average, 48% of the variance of pigments and 50% of the variance of wind stress remained unexplained in this analysis.

Pigment-wind correlations were significant in some squares along the four transects but only slightly more often than expected by chance (1 of the 27 coastal squares or 3 of the 70 oceanic squares, at a probability of 0.05). Seasonal correlations were significant at three and one coastal squares for alongshore and offshore wind stress, respectively, and at eight and two oceanic squares for wind stress and Ekman upwelling, respectively (Figure 10a). Interannual correlations were significant at five and six coastal squares for alongshore and offshore wind stress, respectively, and at seven and eight oceanic squares for wind stress and Ekman upwelling, respectively (Figure 10b). Causal relationships between pigments and winds are suggested by spatial clustering of significant and nearly significant correlations, with pigments lagging winds by up to a month. These patterns can also be seen by comparing space-time plots of pigments and winds (Figures 4-7).

Coastal pigments and winds. Along the coast of central Mexico (105-100°W) the spring maximum in phytoplankton pigments was associated with strong alongshore winds (Figure 4, top). However, the secondary fall maximum occurred during a time of low alongshore wind stress. The interannual decline in pigment concentration beginning in 1982 was associated with a slight weakening of alongshore wind stress (Figure 4, bottom).

At the Gulf of Tehuantepec (96-94°W) the winter maximum

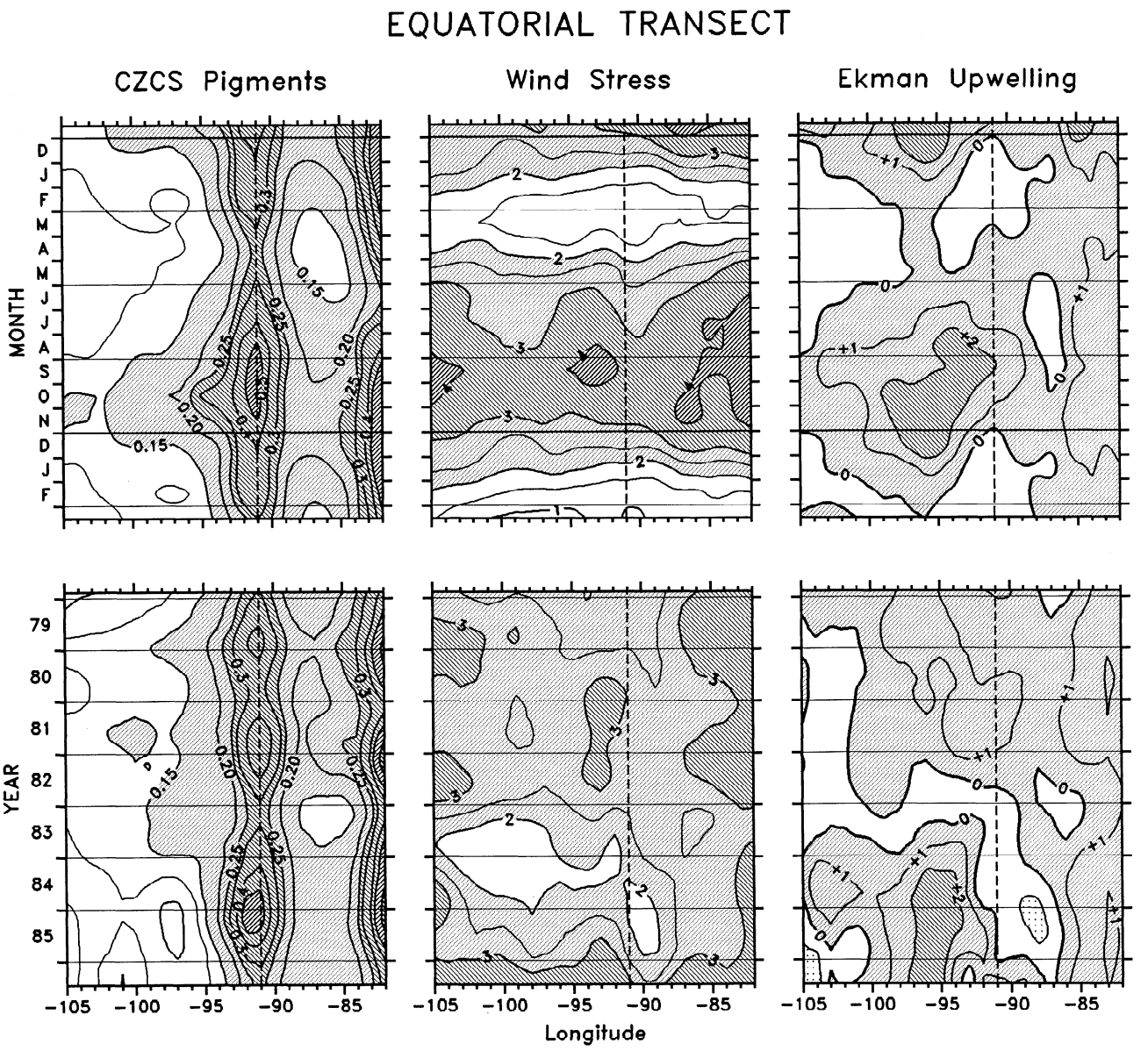

Figure 6. (top) Seasonal (mean residuals from double 13-month running mean) and (bottom) interannual (double 13-month running mean) variability of monthly mean CZCS phytoplankton pigment concentration (in milligrams per cubic meter), wind stress (10^{-2} N m^{-2}), and Ekman upwelling velocity (10^{-5} m s^{-1}) in 1° squares along the equatorial transect. Dashed line marks the Galapagos Islands at 91°W.

in phytoplankton pigments was associated with strong offshore winds (Figure 4, top). This relationship extended 300 km offshore on the 95°W transect, where the late fall pigment maximum was associated with strong southward wind stress. This result is not illustrated here, although it is reflected in the significant correlation with wind stress at 13-14°N (Figure 10a).

At the Gulf of Papgayo (86°W) and Gulf of Panama (79°W), winter-spring maxima in phytoplankton pigments appeared to be associated with strong offshore winds (Figure 4, top). However, secondary maxima beginning in late summer and extending through fall occurred during a time of weak offshore winds, so the seasonal pigment-wind correlations were not quite significant (Figure 10a).

The 1982-1983 decline in phytoplankton pigments in the Gulf of Tehuantepec was associated with weak offshore wind stress during winter 1982-1983 (Figure 4, bottom). However, offshore winds in the Gulfs of Papagayo and Panama were stronger than normal during late 1982 and 1983, so that the interannual correlations between pigments and local winds were negative (Figure 10b).

Oceanic pigments and winds. Along the countercurrent transect, seasonal variability of wind stress was much greater than interannual variability (Table 1). The seasonal cycle of phytoplankton pigment concentration, however, was only nearly significantly correlated with winds at 96-95°W (Figure 10a). West of the Costa Rica Dome (89°W), Ekman upwelling occurred during summer-fall, although it was very weak to the

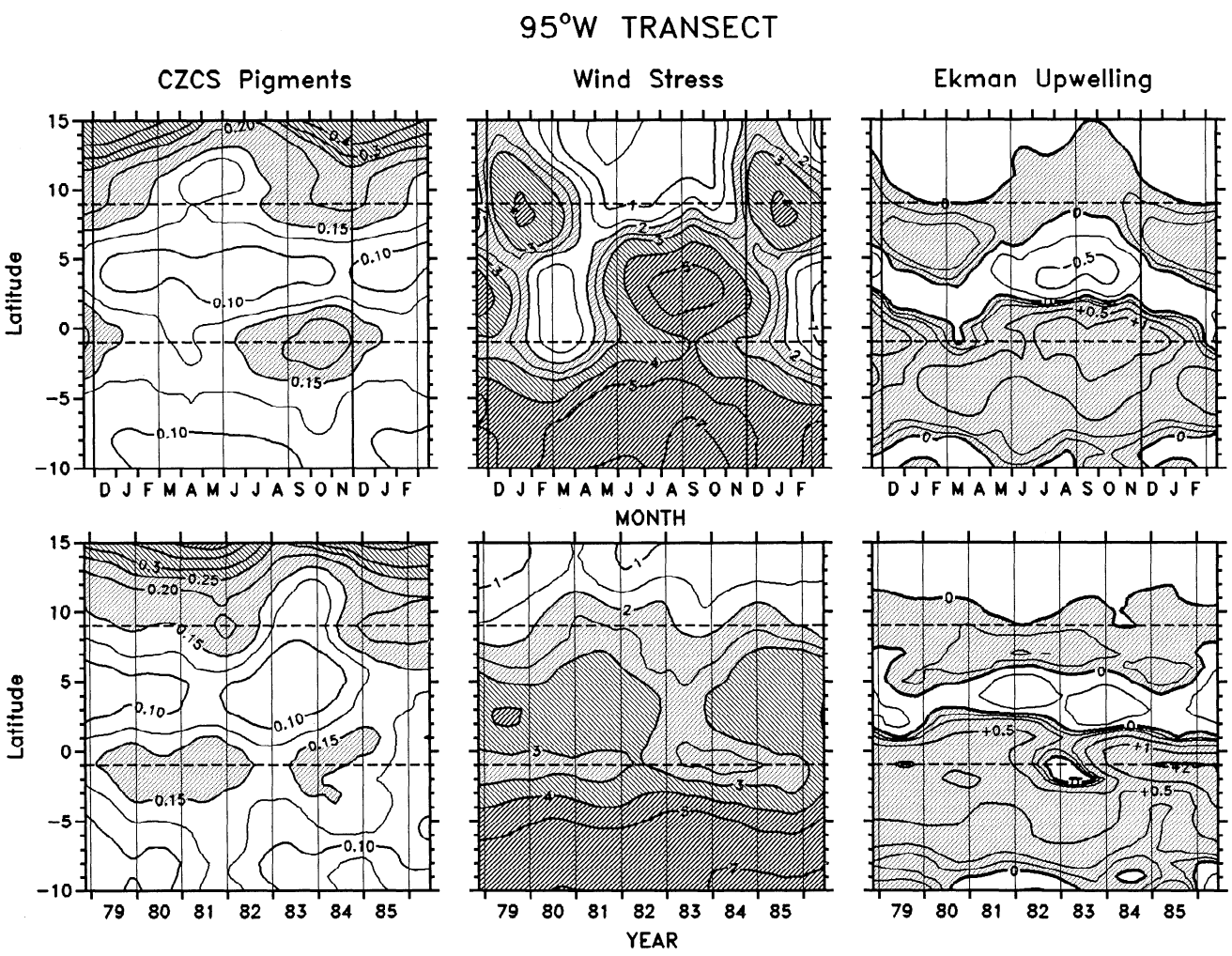

Figure 7. (top) Seasonal (mean residuals from double 13-month running mean) and (bottom) interannual (double 13-month running mean) variability of monthly mean CZCS phytoplankton pigment concentration (in milligrams per cubic meter), wind stress (10^{-2} N m^{-2}), and Ekman upwelling velocity (10^{-5} m s^{-1}) in 1° squares along the 95°W transect. Dashed lines mark the equatorial transect at 1°S and the countercurrent transect at 9°N.

west of 95°W. At this time the ITCZ was north of the countercurrent transect and the trade winds at 9°N were southwesterly and relatively weak. Wind stress reached a secondary maximum in September, when the ITCZ is farthest north and the southeast trades at 9°N are strongest. Pigment concentration declined as downwelling began in December-January. In the region of the Costa Rica Dome (92-87°W), two seasonal pigment maxima occurred just before and after a winter maximum in wind stress and Ekman upwelling.

Interannual pigment-wind correlations along the countercurrent transect tended to be negative (Figure 10b). The interannual decrease of phytoplankton pigments during 1982-1983, especially east of 95°W along this transect, was associated with increased wind stress and Ekman upwelling.

Along the equatorial transect the seasonal cycle of phytoplankton pigments was strongly correlated with wind stress and Ekman upwelling. These correlations decreased to insignificant levels east of 85°W for wind stress and east of 93°W for Ekman upwelling (Figure 10a). To the west of the Galapagos (92-89°W) the fall pigment maximum occurred when the southeast trade winds were seasonally strong (Figure 5, top). Near the coast of Ecuador, the fall-winter pigment maximum lagged the fall wind maximum by 2-3 months. Wind stress and Ekman upwelling decreased during 1982-1983. However, to the west of the Galapagos, CZCS pigment concentration actually increased, resulting in negative interannual correlations between pigments and Ekman upwelling (Figure 10b). At the Galapagos, winds remained weak during 1984-1985, while pigments increased. Interannual pigment-wind correlations were strongly positive only to the east of the Galapagos along the equatorial transect.

Along the 95°W transect the seasonal cycle of phytoplankton pigments near the equator was correlated with wind stress and Ekman upwelling; the fall pigment maximum followed a summer-fall wind maximum. South of the equator, seasonal variability of pigments was less, although a weak fall pigment maximum was associated with maximum wind stress and Ekman upwelling. North of the equator, the band of Ekman upwelling beneath the ITCZ migrates seasonally between 6°N in March and 11°N in September (Figure 7, top). Therefore the seasonal wind cycles to the north and south of the mean latitude of the ITCZ (9°N, the latitude of the countercurrent transect)

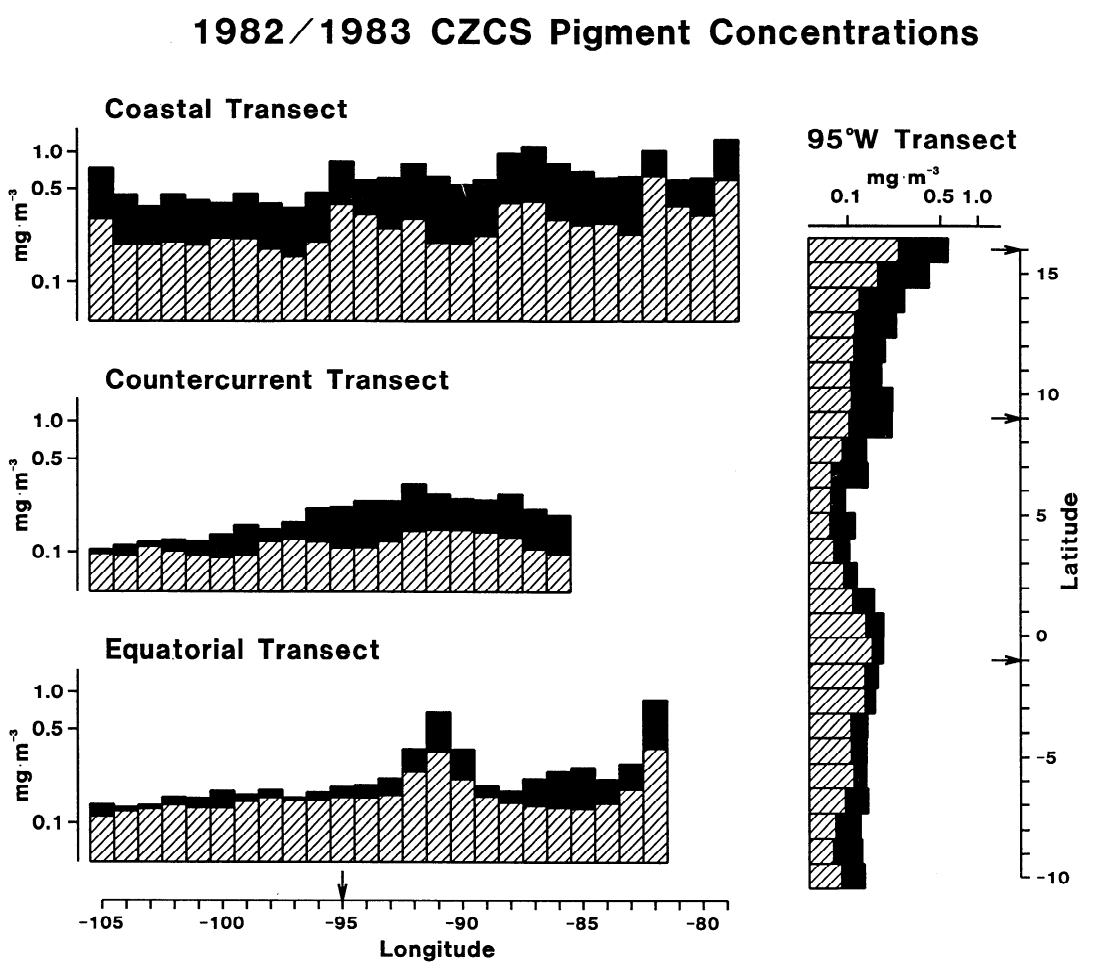

Figure 8. Effect of El Niño 1982-1983 on monthly mean CZCS pigment concentration (in milligrams per cubic meter) in 1° squares along coastal, countercurrent, equatorial, and 95°W transects in the eastern tropical Pacific. Top of solid bar is maximum concentration in the smoothed interannual time series during 1982, and hatched bar is the minimum concentration during 1983. The difference of the log-transformed values represents the relative decrease during El Niño 1982-1983.

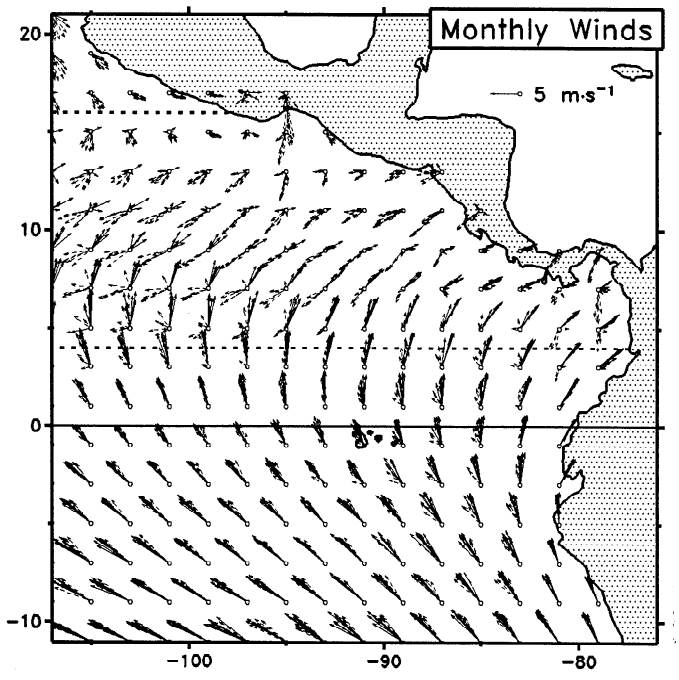

are out of phase. Seasonal variability of pigments was very low on the southern side of the ITCZ. On the northern side the spring minimum and fall maximum of phytoplankton pigments occurred during the seasonal wind reversals, just after the seasonal minimum and maximum of Ekman upwelling.

Wind stress was reduced along 95°W, north of 2°S, during 1982-1983 (Figure 7, bottom). The minimum in phytoplankton pigment concentration, which progressed from winter 1982-1983 at the equator to late 1983 at 13°N, was associated with a similarly progressive wind stress minimum to the north of the equator. Ekman upwelling decreased during 1982-1983 only near the equator.

Discussion and Conclusions

The time series derived from the monthly composite CZCS pigment estimates provide an unprecedented view of spatial-

Figure 9. Monthly mean wind velocities (in meters per second), 1960-1992, from Comprehensive Ocean-Atmosphere Data Set Monthly Summary Trimmed Groups Release 1a data. Solid vectors are May-October; dashed vectors, November-April.

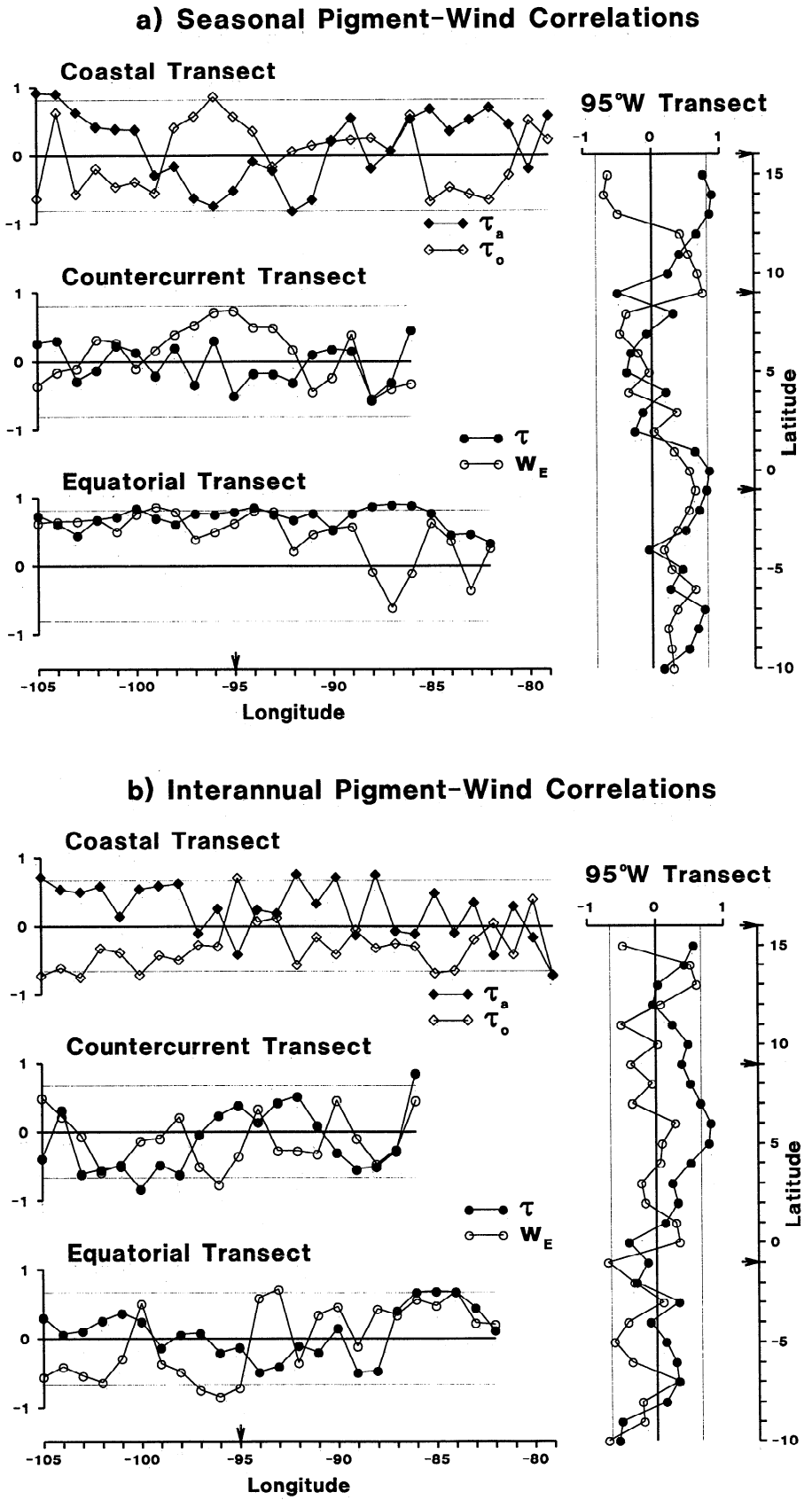

Figure 10. (a) Seasonal correlations r between monthly mean CZCS pigment concentration and wind variables: alongshore wind stress τ_a and offshore wind stress τ_o in the coastal transect and total wind stress τ and Ekman upwelling w_E in the oceanic transects. The critical value for r is 0.81 for P(no correlation)=0.05 and 4 d.f. (b) Interannual correlations r between monthly mean CZCS pigment concentration and wind variables: alongshore wind stress τ_a and offshore wind stress τ_o in the coastal transect and total wind stress τ and Ekman upwelling w_E in the oceanic transects. The critical value for r is 0.66 for P(no correlation)=0.05 and 7 d.f.

temporal variability in the ETP. CZCS data yield a biased estimate of euphotic zone pigment concentration [*Smith*, 1981], which is not always a reliable estimate of phytoplankton biomass, let alone productivity [*Balch et al.*, 1992]. With this caveat, inferences about phytoplankton production can be made from the above results. Changes in phytoplankton biomass, as represented by pigment concentration, are the result of net productivity minus losses due to advection, vertical mixing, grazing, and sinking. Winds affect only some of these processes. Wind-driven upwelling and vertical mixing bring nutrients into the euphotic zone. Nitrate limits primary productivity in regions of the ETP where iron is adequate for nutrient uptake [*Barber and Chavez*, 1991].

Grazing and sinking losses of phytoplankton are not directly influenced by winds, but wind-driven surface currents and vertical mixing cause local changes due to advective and diffusive processes. Advection could influence CZCS pigment time series in the equatorial transect, which lies along the axis of the South Equatorial Current. However, temporal variations of pigments and wind stress were highly coherent along this transect (Figure 11). Therefore advection should not have had a great effect on correlations between pigments and local winds because upstream wind effects on advected pigments were coherent with local pigment variations driven by local winds.

The regions of high pigment concentration observed in the 1° square transects are coastal and oceanic upwelling centers. Pigment concentration along the coast of central Mexico was correlated with alongshore, equatorward wind stress, which drives coastal upwelling in eastern boundary current systems. *Strub et al.* [1990] found significant correlations between CZCS pigment concentration and upwelling favorable, alongshore wind stress in the strong coastal upwelling region of central and northern California (35-45°N).

In contrast, pigment concentration in the Gulf of Tehuantepec was correlated with offshore wind stress. The seasonal correlations were nearly significant in the Gulfs of Papagayo and Panama. At these locations, strong winter winds blow through mountain passes from the Gulf of Mexico [*McCreary et al.*, 1989]. Monthly averaged winds and pigments may not fully capture these wind events and their effects on phytoplankton production. Gulf of Tehuantepec "Norte" winds

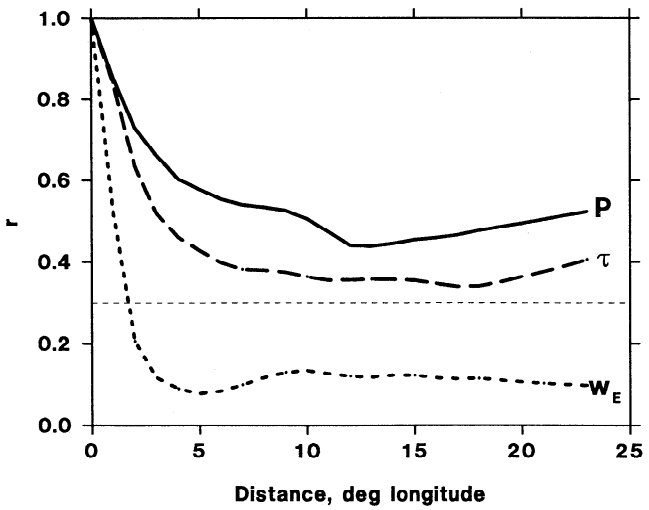

Figure 11. Spatial coherence (r versus distance) of monthly mean CZCS pigment concentration P, wind stress τ, and Ekman upwelling w_E in 1° squares along the equatorial transect.

last 3 to 4 days and may attain speeds >20 m s^{-1}. Cold, subsurface water is brought to the surface by intense vertical mixing beneath the wind jet and upwelling beneath the cyclonic (divergent) eastern flank of the jet [*Barton et al.*, 1993].

The oceanic regions of high pigment concentration in the ETP are also centers of upwelling [*Fiedler et al.*, 1991]. Equatorial upwelling is driven by the westward component of the SE trade winds, which forces divergent, poleward Ekman transport of surface waters [*Wyrtki*, 1981]. An island effect is reflected in the strong upwelling to the west of the Galapagos and the weak upwelling or downwelling to the east (Figure 6).

The Costa Rica Dome is also a center of oceanic upwelling. The thermocline and nutricline are very close to the surface and well within the euphotic zone, although they never break the surface, as in coastal upwelling regions [*Broenkow*, 1965; *Fiedler et al.*, 1991]. The seasonal cycle shows pigment maxima in both spring and fall, under seasonally opposite wind regimes (Figure 5, top). The spring bloom is clearly related to local Ekman upwelling, but the fall bloom cannot be explained by local winds. The time series analysis has at least defined the distinct seasonal cycle at the Dome. In individual or monthly composite CZCS images it is often difficult to differentiate pigment maxima along the coast at the Gulf of Papagayo and at the adjacent Costa Rica Dome. Weak Ekman upwelling occurs to the west of the Costa Rica Dome, where a fall pigment maximum follows a summer-fall Ekman upwelling maximum. This relationship becomes weaker as upwelling decreases to the west.

Interannual variability was dominated by the 1982-1983 El Niño event along all transects. This extreme event probably biased the relative magnitude of seasonal and interannual variability in the CZCS pigment data. The coherence of interannual variability in the CZCS pigment time series throughout the ETP raises the possibility that this variability was the result of instrumental error. Systematic error in the pigment calibration or in correction of the decay of radiometric sensitivity [*Evans and Gordon*, 1994] could produce apparent interannual variability. In a comparison of satellite-derived and shipboard pigment estimates, *Balch et al.* [1992] found that the CZCS consistently underestimated pigment concentrations at values <1 mg m^{-3}, as was true in the present study. They found no temporal trend for this error and, in fact, their results suggest a positive bias of CZCS pigment estimates during 1983 [*Balch et al.*, 1992, Figure 8c]. Aerosols introduced by the eruption of El Chichón in April 1982 should have had little effect on CZCS pigment estimates [*Gordon and Castana*, 1988]. Finally, instrumental bias cannot account for the observed spatial differences in the timing and magnitude of the CZCS pigment decline during 1983.

Pigment-wind relationships on the interannual scale were, in some cases, analogous to seasonal relationships. For example, pigments increased seasonally and interannually with alongshore wind stress along the central coast of Mexico and with offshore wind stress at the Gulf of Tehuantepec. In other cases, interannual relationships were qualitatively different than seasonal relationships. For example, seasonal increases in pigment concentration followed strong offshore winds in the Gulfs of Papagayo and Panama. Offshore winds were anomalously strong during winter 1982-1983, but pigment concentration decreased. This could have been caused by increased advective loss of the spring bloom or by reduction of the fall bloom, which normally occurred at these locations during a period of relatively weak winds.

A fall pigment maximum was associated with high wind stress and Ekman upwelling along the equatorial transect and the countercurrent transect west of the Costa Rica Dome. During the 1982-1983 El Niño, wind stress and Ekman upwelling decreased along the equatorial transect, but pigment concentration decreased markedly only at the Galapagos and to the east, toward the coast of Ecuador. At the same time, wind stress and Ekman upwelling increased along the countercurrent transect, while pigments decreased. Remotely forced depression of the thermocline during this event [*McPhaden and Hayes*, 1990] countered the effects of increased local winds on phytoplankton productivity by deepening the nutricline [*Barber and Chavez*, 1986; *Halpern and Feldman*, 1994]. Although nutrients were not depleted in eastern equatorial surface water during the 1982-1983 El Niño, low iron levels may have limited the ability of phytoplankton to take up the available nitrate [*Barber and Chavez*, 1991].

The analysis of CZCS pigment estimates showed that the effect of El Niño on phytoplankton production was low to the west of the Galapagos. The effect increased both to the east and to the north toward the coast of Central America. This was a surprising result that has not been apparent in attempts to compile limited regional observations [e.g., *Barber and Chavez,* 1986]. Inadequate coverage by the CZCS precluded an analysis of monthly phytoplankton variability west of 105°W. Recent analyses of CZCS pigment concentrations in the equatorial Pacific have had to use means for areas > 1° square or periods > 1 month [*Halpern and Feldman*, 1994; C. L. Leonard and C. R. McClain, Assessment of interannual variation (1979-1986) in pigment concentrations in the tropical Pacific, submitted to *Journal of Geophysical Research*, 1994]. Both of these studies showed a greater pigment decrease during the 1982-1983 El Niño in the central equatorial Pacific (180-140°W) than in the region immediately to the west of the Galapagos, but they failed to resolve a seasonal signal in either region.

New ocean color sensors like the sea-viewing wide field-of-view sensor (SeaWIFS) and the moderate-resolution imaging spectrometer (MODIS) promise to provide a more complete data set that will allow monitoring and analysis of global phytoplankton variability. This study has shown that an ocean color sensor data set can yield useful estimates of spatial and temporal variability of apparent phytoplankton production. Seasonal variabilities of CZCS pigments and winds in the eastern tropical Pacific were at least as great as interannual variability, even during a period dominated by the 1982-1983 El Niño. Seasonal cycles and interannual changes of pigments were linked to wind-driven processes that affect primary productivity. Ultimately, we hope to use such data in studies of the spatial and temporal variability of habitats and populations of fish, birds, and marine mammals.

Acknowledgements. I thank Gene Feldman and Norm Kuring (NASA) for providing the CZCS monthly composite pigment data and Dan Cayan (SIO) and Steve Worley (NCAR) for providing COADS wind data. Valerie Philbrick and John Steger provided image-processing support during the initial stages of this analysis. Ken Raymond drafted Figure 1. I thank Ted Strub and Andy Thomas for comments on an initial draft of this manuscript, Valerie Philbrick for editorial assistance, two anonymous reviewers for valuable comments, and Steve Reilly and Mike Laurs for continuing support.

References

Balch, W., R. Evans, J. Brown, G. Feldman, C. McClain, and W. Esaias, The remote sensing of ocean primary productivity: Use of a new data compilation to test satellite algorithms, *J. Geophys. Res., 97*, 2279-2293, 1992.

Barber, R. T., and F. P. Chavez, Ocean variability in relation to living resources during the 1982/83 El Niño, *Nature, 319*, 279-285, 1986.

Barber, R. T., and F. P. Chavez, Regulation of primary productivity rate in the equatorial Pacific, *Limnol. Oceanogr., 36*, 1803-1815, 1991.

Barton, E. D., M. L. Argote, J. Brown, P. M. Kosro, M. Lavin, J. M. Robles, R. L. Smith, A. Trasviña, and H. S. Velez, Supersquirt: Dynamics of the Gulf of Tehuantepec, Mexico, *Oceanography, 6*(1), 23-30, 1993.

Broenkow, W. W., The distribution of nutrients in the Costa Rica Dome in the eastern tropical Pacific Ocean, *Limnol. Oceanogr., 10*, 40-52, 1965.

Chelton, D. B., Statistical reliability and the seasonal cycle: Comments on "Bottom pressure measurements across the Antarctic Circumpolar Current and their relation to the wind, *Deep Sea Res., Part A, 29*, 1381-1388, 1982.

Cowles, T. J., R. T. Barber, and O. Guillen, Biological consequences of the 1975 El Niño, *Science, 195*, 285-287, 1977.

Dandonneau, Y., Surface chlorophyll concentration in the tropical Pacific Ocean: An analysis of data collected by merchant ships from 1978 to 1989, *J. Geophys. Res., 97*, 3581-3591, 1992.

Delcroix, T., Seasonal and interannual variability of sea surface temperatures in the tropical Pacific, 1969-1991, *Deep Sea Res. I, 40*, 2217-2228, 1993.

Dessier, A., and J. R. Donguy, Planktonic copepods and environmental properties of the eastern equatorial Pacific: seasonal and spatial variations, *Deep Sea Res., Part A, 32*, 1117-1133, 1985.

Evans, R. H., and H. R. Gordon, Coastal zone color scanner "system calibration": A retrospective examination, *J. Geophys. Res., 99*, 7293-7308.

Feldman, G., D. Clark, and D. Halpern, Satellite color observations of the phytoplankton distribution in the eastern equatorial Pacific during the 1982-1983 El Niño, *Science, 226*, 1069-1071, 1984.

Feldman, G. C., Variability of the productive habitat in the eastern equatorial Pacific, *Eos, Trans. AGU, 67*, 106-108, 1986.

Fiedler, P. C., Seasonal climatologies and variability of eastern tropical Pacific surface waters, *NOAA Tech. Rep. NMFS, 109*, 65 pp., 1992.

Fiedler, P. C., V. Philbrick, and F. P. Chavez, Oceanic upwelling and productivity in the eastern tropical Pacific, *Limnol. Oceanogr., 36*, 1834-1850, 1991.

Fiedler, P. C., F. P. Chavez, D. W. Behringer, and S. B. Reilly, Physical and biological effects of Los Niños in the eastern tropical Pacific, 1986-1989, *Deep Sea Res., Part A, 39*, 199-219, 1992.

Gordon, H. R. and D. J. Castana, Coastal Zone Color Scanner atmospheric correction: Influence of El Chichón, *Appl. Opt., 27*, 3319-3322, 1988.

Glynn, P. W. (Ed.), *Global Ecological Consequences of the 1982-83 El Niño-Southern Oscillation*, Elsevier, New York, 1990.

Halpern, D., and G. C. Feldman, Annual and interannual variations of phytoplankton pigment concentration and upwelling along the Pacific equator, *J. Geophys. Res., 99*, 7347-7354, 1994.

Hsieh, W. W., and G. J. Boer, Global climate change and ocean upwelling, *Fish. Oceanogr., 1*, 333-338, 1992.

Large, W. G., and S. Pond, Open ocean momentum flux measurements in moderate to strong winds, *J. Phys. Oceanogr., 11*, 324-336, 1981.

McClain, C. R., G. Fu, M. Darzi, and J. K. Firestone, PC-

SEAPAK user's guide, version 4.0, *NASA Tech. Mem., TM 104557*, 332 pp., 1992.

McCreary, J. P., H. S. Lee, and D. B. Enfield, The response of the coastal ocean to strong offshore winds: With application to circulations in the Gulfs of Tehuantepec and Papagayo, *J. Mar. Res., 47*, 81-109, 1989.

McPhaden, M. J., and S. P. Hayes, Variability in the eastern equatorial Pacific Ocean during 1986-1988, *J. Geophys. Res., 95*, 13,195-13,208, 1990.

Rojas de Mendiola, B., Seasonal phytoplankton distribution along the Peruvian coast, in *Coastal Upwelling, Coastal Estuarine Sci.*, vol. 1, edited by F. A. Richards, pp. 348-356, AGU, Washington, D. C., 1981.

Schreiber, R. W., and E. A. Schreiber, Central Pacific seabirds and the El Niño Southern Oscillation: 1982 to 1983 perspectives, *Science, 225*, 713-716, 1984.

Smith, R. C., Remote sensing and depth distribution of ocean color, *Mar. Ecol. Prog. Ser., 5*, 359-361, 1981.

Strub, P. T., C. James, A. C. Thomas, and M. R. Abbott, Seasonal and nonseasonal variability of satellite-derived surface pigment concentration in the California Current, *J. Geophys. Res., 95*, 11,501-11,530, 1990.

Thomas, A. C., F. Huang, P. T. Strub, and C. James, Comparison of the seasonal and interannual variability of phytoplankton pigment concentrations in the Peru and California Current systems, *J. Geophys. Res., 99*, 7355-7370, 1994.

Trillmich, F., and D. Limberger, Drastic effects of El Niño on Galapagos pinnipeds, *Oecologia, 67*, 19-22, 1985.

Valdivia, J. E., The anchoveta and El Niño, *Rapp. P.-V. Réun. Cons. Int. Explor. Mer, 173*, 196-202, 1978.

Woodruff, S. D., R. J. Slutz, R. L. Jenne, and P. M. Steurer, A comprehensive ocean-atmosphere data set, *Bull. Am. Meteorol. Soc., 68*, 1239-1250, 1987.

Wyrtki, K., An estimate of equatorial upwelling in the Pacific, *J. Phys. Oceanogr., 11*, 1205-1214, 1981.

P. C. Fiedler, National Marine Fisheries Service, Southwest Fisheries Science Center, P. O. Box 271, La Jolla, CA 92038-0271. (e-mail: paul@caliban.ucsd.edu)

(Received December 13, 1993; revised May 2, 1994; accepted July 12, 1994.)